Positronium formation in the ground and excited states ($n=2$ levels) in a positron-negative hydrogen-ion collision

D. Ghosh and C. Sinha
Theoretical Physics Department, Indian Association for the Cultivation of Science, Kolkata 700032, India
(Received 12 January 2004; published 21 May 2004)

An approach has been proposed and developed to study the positronium (Ps) formation cross sections in the ground and excited $n=2$ levels for the exothermic reaction in a positron-negative hydrogen-ion (H^-) collision in the framework of Coulomb distorted eikonal approximation. Both the differential cross sections (DCS) as well as integrated cross sections [partial total cross sections (TCS)] have been investigated for the 1*s*, 2*s*, and 2*p* states in a broad energy range, e.g., 1–200 eV. For lower incident energy, the Ps formation in the 2*p* state is found to dominate over the 1*s* and 2*s* states while for the higher incident energy, the formation to ground state (1*s*) dominates the other two states. Present results have been compared with other existing theoretical results where available in the absence of any experimental data. Both the DCS and the partial TCS results are found to agree quite satisfactorily with the coupled pseudostate results of McAlinden *et al.* [Phys. Rev. A **65**, 032715 (2002)] in the low-energy range 1–10 eV. At higher incident energies, the present results are always lower than the Coulomb Born and orthogonalized Coulomb Born results of Basu Choudhury *et al.* [Phys. Rev. A **33**, 2358 (1986)] and Straton *et al.* [Phys. Rev. A **44**, 7335 (1991)], respectively. The present DCS (1*s*,2*s*) exhibits double peak structure at high incident energy that could be attributed to higher-order effects. The signature of the present double peak structure which is totally absent in the Coulomb Born approximation or in the orthogonalized Coulomb Born approximation becomes more prominent with increasing incident energy.

DOI: 10.1103/PhysRevA.69.052717 PACS number(s): 34.70.+e

I. INTRODUCTION

The increasing advancement in the detection techniques as well as in the availability of intense monoenergetic positron beams have made it possible to perform much more sophisticated experiments in positron-atom scattering. Of late, the emphasis on the experimental determinations of total cross sections for the scattering of positrons by different gas targets has shifted to the measurement of partial cross sections [1–6] for the various inelastic channels, among which the positronium (Ps) formation capture channel is of utmost importance [7–9]. These measurements have stimulated much theoretical investigations [7–23] for this particular rearrangement process using different gas targets.

The importance of the process of Ps formation in ground or excited states in positron- negative hydrogen-ion (H^-) collisions has already been emphasized in the earlier theoretical works [21–23] on this process, particularly in the field of astrophysics, since the concentration of the H^- ion in the transition regions of planetary nebulae [22] is supposed to be quite large for the Ps formation reactions thereby making significant contributions in understanding the detected feature of the spectrum of the electron positron annihilation radiation observed to be coming from the direction of the galactic center and also from solar flares [7].

Since the ionization potential of the H^- ion is much less than the binding energy of the ground and the few excited states of positronium, the Ps formation channel is open even at zero positron energy for these states, i.e., the reaction is exothermic. This gives added incentive for the study of such process theoretically. Regarding experimental situation, to our knowledge, there is no measurement for the Ps formation with H^- ionic target as yet, though the breakthrough in the study of electron-negative ion scattering indicates [24] the bright future for the corresponding measurements for positron impact.

As regards other theoretical works on this particular process, to our knowledge, two perturbative calculations in the Coulomb Born approximation (CBA) and in the orthogonalized Coulomb Born approximation (OCBA) due to Basu Choudhury *et al.* [23] and Straton *et al.* [22], respectively, exist in the literature, the other one is due to McAlinden *et al.* [21] who studied the process in the framework of coupled pseudostate approach (CPA), using 19 Ps pseudostates centered on the positron. Nevertheless, the latter calculations concentrate on the low incident (positron) energy only.

The present theoretical work deals with the study of the differential as well as total Ps formation cross sections for capture to ground and excited (2*s*,2*p*) states in e^+-H^- ion collisions. The present calculations have been performed in the framework of Coulomb distorted eikonal approximation (CDEA) that takes account of higher-order effects which is essential for a rearrangement process especially at high incident energies where the first Born approximation is not supposed to be adequate. Further, for an ionic target, as happens to be the present case, the long-range Coulomb interaction between the projectile and the target ion in the initial channel must be taken into account in order to have a reasonable estimate for the capture cross sections.

Expecting that the major contribution to excited state capture comes from the $n=2$ level at higher incident energies, the main emphasis is given on the calculation of Ps formation to the ground and excited $n=2$ level (2*s*,2*p*) only, in the present work. Further, assuming that the formation cross section falls off as n^{-3} at intermediate and high incident energies; the present calculation also allows the prediction of an

estimate of the total Ps formation cross sections in these energy regimes. Since the electron affinity of the H^- ion is less than the binding energy of the first few excited states of the Ps atom, we present our results starting from the incident energy 1 eV onwards for ground or excited state $(2s,2p)$ capture. The present results have been compared with the existing theoretical results (where available), in the absence of any experimental data. In the present work we have used atomic units (a.u.) throughout except for the integral cross sections which will be expressed in the unit of πa_0^2.

II. THEORY

The expressions for the post and the prior forms of the amplitude for Ps formation in the process $e^+ + H^- \rightarrow (e^+e)(1s,2s,2p) + H(1s)$ are given as

$$T_{if}^{post} = \langle \psi_f | V_f | \Psi_i^+ \rangle, \tag{1a}$$

$$T_{if}^{prior} = \langle \Psi_f^- | V_i | \psi_i \rangle, \tag{1b}$$

where V_i and V_f are the perturbations in the initial and final channels, respectively. In Eqs. (1a) and (1b) Ψ_i^+ or Ψ_f^- is an exact solution of the four body problem satisfying the outgoing or incoming wave boundary condition, respectively. In the present work we have chosen the post form (1a) since for such rearrangement processes the post form of the amplitude might be more appropriate than the prior form [25]. Thus in the present case, Ψ_i^+ satisfies the equation

$$(H - E)\Psi_i^+ = 0, \tag{2}$$

where the total Hamiltonian of the present $e^+ - H^-$ ion system is written as

$$H = H_0 + \frac{Z_t}{r_1} - \frac{Z_t}{r_2} - \frac{Z_t}{r_3} - \frac{1}{r_{12}} - \frac{1}{r_{13}} + \frac{1}{r_{23}}, \tag{3}$$

$Z_t(=1)$ being the charge of the target nucleus. $\vec{r}_1$, $\vec{r}_2$, and $\vec{r}_3$ are the position vectors of the incoming positron "1" and the two bound electrons "2" and "3", respectively, with respect to the target nucleus; $\vec{r}_{12} = \vec{r}_1 - \vec{r}_2$, $\vec{r}_{13} = \vec{r}_1 - \vec{r}_3$, $\vec{r}_{23} = \vec{r}_2 - \vec{r}_3$. The full kinetic-energy operator H_0 in Eq. (3) is given by

$$H_0 = -\tfrac{1}{2}\nabla_1^2 - \tfrac{1}{2}\nabla_2^2 - \tfrac{1}{2}\nabla_3^2. \tag{4}$$

The binding energy relation for the process is given as, $\frac{1}{2}K_i^2 + \varepsilon_{h^-} = (K_{ps}^2/2) + \varepsilon_{ps} + \varepsilon_h$; K_i being the initial momentum of the incident positron, ε_{h^-} is the binding energy, and ϕ_i is the ground-state wave function of the negative hydrogen ion; K_{ps} being the final momentum of the positronium atom and ε_{ps} and ε_h are the binding energies of the final Ps and H atoms, respectively.

The asymptotic initial channel wave function ψ_i of the e^+-H^- ion system satisfies the following Schrodinger equation:

$$\left[H_0 - \frac{Z_t}{r_2} - \frac{Z_t}{r_3} + \frac{1}{r_{23}} + \frac{1}{r_1} \right] \psi_i = E_0 \psi_i, \tag{5}$$

where the solution ψ_i of Eq. (5) is the product of the screened Coulomb wave function [26] and the bound-state wave function of the H^- ion, i.e.,

$$\psi_i(\vec{r}_1) = (2\pi)^{-3/2} \exp\left(\frac{\pi\alpha_i}{2} \right) \Gamma(1 - i\alpha_i) \times \exp(i\vec{K}_i \cdot \vec{r}_1)\, {}_1F_1[i\alpha_i, 1; i(K_i r_1 - \vec{K}_i \cdot \vec{r}_1)]\, \phi_i(\vec{r}_2, \vec{r}_3), \tag{6}$$

where $\alpha_i = -1/K_i$. The ground-state wave function of the H^- ion is given by Chandrasekhar [27] as

$$\phi_i(\vec{r}_2, \vec{r}_3) = \frac{1}{4\pi} N (e^{-\alpha r_1} e^{-\beta r_2} + e^{-\beta r_1} e^{-\alpha r_2}), \tag{7}$$

with $N = 0.3948$, $\alpha = 1.039\,25$, and $\beta = 0.283\,09$. The ground-state energy of the H^- ion for this wave function [27] is $E = -0.513$ a.u.

The exact initial-state wave function Ψ_i^+ occurring in Eq. (1a) has been approximated in the framework of eikonal approximation as

$$\Psi_i^+ = \psi_i \exp\left[i\eta_i \int_{-\infty}^{z_1} \left(\frac{1}{r_1} - \frac{1}{r_{12}} \right) dz_1' \right], \tag{8}$$

with $\eta_i = 1/K_i$. The integration variable z_1' in Eq. (8) is the z component of the vector $\vec{r}_1$. To evaluate the phase integral occurring in Eq. (8), we choose the polar axis in the direction of $\vec{K}_i$ and the result is

$$\Psi_i^+ = \psi_i(\vec{r}_1)(r_1 - z_1)^{i\eta_i}(r_{12} - z_{12})^{-i\eta_i}. \tag{9}$$

In constructing the initial channel wave function Ψ_i^+ in Eq. (1a), an assumption is made (for the sake of simplicity) that the incident positron is distorted only by the active electron 2 to be captured, while the role of the passive electron 3 is only to screen the nucleus by its negative charge cloud, thereby reducing the four-body problem to a three-body one in the final channel. This approximation should be quite legitimate for intermediate and high incident positron energies. The final-state wave function ψ_f in Eq. (1a) is chosen as

$$\psi_f = e^{i\vec{K}_f \cdot \vec{S}} \phi_{ps} \phi_h, \tag{10}$$

where $\vec{K}_f$ is the final momentum of the Ps atom; $\vec{S} = (\vec{r}_1 + \vec{r}_2)/2$; ϕ_{ps} and ϕ_h are the bound-state wave functions of the Ps and H atom, respectively. In view of Eqs. (1a), (3), and (10), the post form of the interaction V_f in Eq. (1a) given as

$$V_f = \frac{Z_t}{r_1} - \frac{Z_t}{r_2} - \frac{1}{r_{13}} + \frac{1}{r_{23}}. \tag{11}$$

Thus in the framework of Coulomb distorted eikonal approximation, the expression for T_{if}^{post} in Eq. (1a) takes the form

$$T_{if} \approx -\frac{\mu_f}{2\pi} C_1 \int e^{-i\vec{K}_f\cdot\vec{S}} \exp(-\lambda_{Ps}|\vec{r}_1-\vec{r}_2|)\exp(-\lambda_H r_3) \times V_f \phi_{H^-}(\vec{r}_2,\vec{r}_3)\exp(i\vec{K}_i\cdot\vec{r}_1)\,{}_1F_1(i\alpha_i,1;i(K_i r_1-\vec{K}_i\cdot\vec{r}_1)) \times (r_1-z_1)^{i\eta_i}(r_{12}-z_{12})^{-i\eta_i} d\vec{r}_1 d\vec{r}_2 d\vec{r}_3, \quad (12)$$

where C_1 involves the normalization constants for the bound and continuum states occurring in Eq. (12); μ_f is the three-body reduced mass in the final channel.

Finally, the TDCS for the Ps formation process of a negative hydrogen ion is given by

$$\frac{d\sigma}{d\Omega} = \frac{v_f}{v_i}|T_{if}|^2. \quad (13)$$

The total cross section σ is obtained by integrating Eq. (13) over the solid angle of the Ps atom, i.e.,

$$\sigma = 2\pi \frac{v_f}{v_i}\int_0^\pi \frac{d\sigma}{d\Omega}\sin\,\theta\, d\theta, \quad (14)$$

where v_i and v_f are the initial and final velocities of the e^+ and Ps, respectively.

To evaluate the transition amplitude in Eq. (12) we use the following contour integral representations of the confluent hypergeometric function as well as the eikonal phase factors occurring in Eq. (12). The confluent hypergeometric function:

$${}_1F_1(i\alpha,1,z) = \frac{1}{2\pi i}\int_{\Gamma_1}^{(0^+,1^+)} p(\alpha,t)\exp(zt)dt, \quad (15)$$

with $\mathrm{p}(\alpha,t)=t^{-1+i\alpha}(t-1)^{-i\alpha}$, Γ_1 is a closed contour encircling the two points 0 and 1 once anticlockwise. At the point where the contour crosses the real axis to the right-hand side of 1, arg "t" and arg "$(t-1)$" are both zero [28]. The eikonal phase factor is of the form

$$y^{\pm(\eta-m)} = \frac{(-1)^{m+1}}{2i\,\sin(\mp\pi i\eta)\Gamma(\mp i\eta\pm m)} \times \int_c (-\lambda)^{\mp i\eta\pm m-1}\exp(\lambda y)d\lambda, \quad (16a)$$

where the contour c has a branch cut from 0 to ∞. To obtain this we have made use of the contour integral representation of the complex Γ function [29].

$$\Gamma(x) = -\frac{1}{2i\,\sin(\pi x)}\int_c (-t')^{x-1}\exp(-t')dt'. \quad (16b)$$

In view of the above two integral representations and carrying out the space integrations in Eq. (12), we arrive at a basic integral of the type (apart from the constants)

$$I_0 \approx \int_{c_1}\int_{c_2}\int_{\Gamma_i} f_1(\lambda_1,\eta_1)f_2(\lambda_2,\eta_2) \times \frac{p(\alpha_i,t_i)}{(q^2+\lambda^2)((|\vec{q}-\vec{q}_1|)^2+\mu_1^2)(|\vec{q}-\vec{q}_2|^2+\mu_2^2)} d\vec{q}\,d\lambda_1 d\lambda_2 dt_i, \quad (17)$$

with $f_1(\lambda_1,\eta_i)=(-\lambda_1)^{-i\eta_i-1}$; $f_2(\lambda_2,\eta_i)=(-\lambda_2)^{i\eta_i-1}$; $\vec{q}_1,\vec{q}_2,\mu_1,\mu_2$ are functions of the initial and final momenta $(\vec{K}_i,\vec{K}_f)$, the initial and final bound state parameters $(\alpha,\beta,\lambda_{ps},\lambda_h)$ as well as the integration variables λ_1,λ_2, and t_i. The actual integral occurring in Eq. (12) may be generated from I_0 by suitable parametric differentiations. The $\vec{q}$ integral in Eq. (17) was performed analytically by Lewis [30] to obtain

$$J_0 = \frac{\pi^2}{\sqrt{\beta'^2-\alpha'\gamma'}}\ln\left[\frac{\beta'+\sqrt{\beta'^2-\alpha'\gamma'}}{\beta'-\sqrt{\beta'^2-\alpha'\gamma'}}\right], \quad (18)$$

with

$$\beta' = \lambda[|\vec{q}_1-\vec{q}_2|^2+(\mu_1+\mu_2)^2]+\mu_2(\lambda^2+q_1^2+\mu_1^2) + \mu_1(\lambda^2+q_2^2+\mu_2^2)$$

and

$$\alpha'\gamma' = [|\vec{q}_1-\vec{q}_2|^2+(\mu_1+\mu_2)^2]\times[q_1^2+(\lambda+\mu_1)^2] \times[q_2^2+(\lambda+\mu_2)^2]. \quad (19)$$

The function J_0 in Eq. (18) involves a logarithmic branch cut [13] and hence in order to avoid complexity in mathematical evaluation, we use the following integral representation [31] for the function J_0:

$$J_0 = 2\pi^2\int_0^\infty \frac{dx}{\alpha' x^2+2\beta' x+\gamma'}, \quad (20)$$

where the product $\alpha'\gamma'$ has been split in such a manner that both α' and γ' are individual linear functions of the integration variables λ_1 and λ_2. By virtue of this choice we can perform λ_1 and λ_2 integrations analytically. In view of Eqs. (17) and (20), we arrive at the following type of integral:

$$J_0 = \int_0^\infty\int_{c_1}\frac{f(\lambda_1,\eta_i)f(\lambda_2,\eta_i)}{(A+B\lambda_1+C\lambda_2+D\lambda_1\lambda_2)}dx\,d\lambda_1\,d\lambda_2, \quad (21)$$

where the contour c_1 refers to the same as that in Eq. (16a).

The λ_1,λ_2 integrations in Eq. (21) have now been performed analytically by the use of residue calculation techniques to obtain finally

$$I_0(t_i,v) \approx -4\pi^2\frac{1}{2\pi i}\int_c\int_0^\infty \frac{1}{A}\left[\frac{B}{A}\right]^{i\eta_i}\left[\frac{C}{A}\right]^{-i\eta_i} \times {}_2F_1(-i\eta_i,i\eta_i,1,z')dx, \quad (22)$$

where $z'=1-(AD/BC)$; ${}_2F_1$ denotes the hypergeometric function with argument z'. We are thus finally left with a two-dimensional integral over x and t_i. The complex integration over t_i has been converted to a real one-dimensional

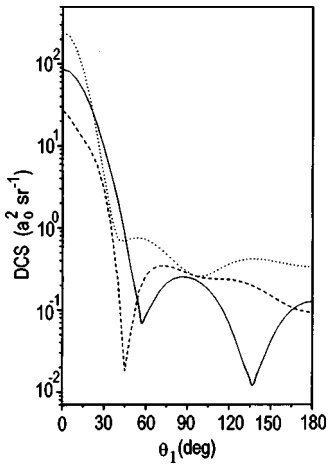

FIG. 1. Differential cross sections (DCS) (in a_0^2 sr^{-1}) for positronium formation in $1s,2s$, and $2p$ states in positron-negative hydrogen-ion collisions for incident energy E_i=5 eV, solid line for $1s$, dashed line for $2s$, and dotted line for $2p$ state.

integral [32] over the range 0 to 1 and the final two-dimensional integral in the transition matrix element [Eq. (1a)] is then evaluated numerically using Gaussian quadrature methods [31].

III. RESULTS AND DISCUSSIONS

We have computed the Ps formation cross sections, both differential and total, for the process $e^+ + H^-(1s) \rightarrow (e^+e)(1s,2s,2p) + H(1s)$ in the framework of CDEA.

Figures 1–3 exhibit the present differential cross sections (DCS) in the ground and excited $(2s,2p)$ states for incident positron energies (E_i) 5 eV, 10 eV, and 25 eV, respectively.

Figure 1 reveals that the Ps formation in all the states $1s$, $2s$, $2p$ is strongly favored in the forward direction. The DCS curve for the $1s$ state (solid) in Fig. 1 shows two distinct minima separated by a broad distinct peak at an angle $\approx 85°$. For the $2s$ state (dashed), on the other hand, the DCS curve shows a very sharp single minimum at $\approx 45°$ followed by a shoulderlike structure, while for the $2p$ state, instead of a distinct minimum, only a kink at around 55°, followed by a broad maximum ($\approx 135°$) are noted. It is also evident from Fig. 1 that at 5 eV, the maximum Ps cross section at extreme forward angles is largest for the $2p$ state and smallest for the $2s$ state while the $1s$ state lies in between. Similar feature was noted by McAlinden *et al.* [21] in their CPA for low scattering angles at a higher incident energy (e.g., 10 eV). For higher scattering angles, on the other hand, the magnitude of the partial DCS follows the order $2p > 2s > 1s$. However some exceptions occurs at extreme backward angles, e.g., in the region $\approx 165° - 180°$. It may be mentioned that in the work of McAlinden *et al.* [21], the figures are presented in a reduced linear scale and as such the finer details of the DCS structure are somewhat suppressed.

In Fig. 2(a), 2(b), and 2(c) we have displayed the present DCS results for the $1s$, $2s$, and $2p$ states, respectively, at E_i=10 eV along with the corresponding results of McAlinden *et al.* [21] for comparison. As may be noted from the

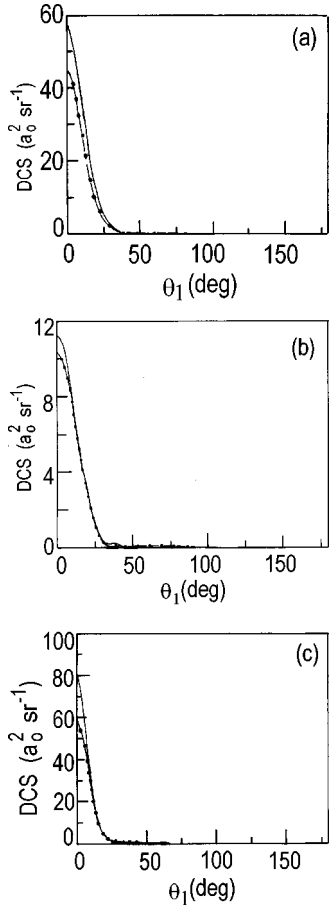

FIG. 2. (a) Ps formation cross sections (DCS) to a $1s$ state for incident energy 10 eV. Dashed dot curve represents present result and the solid curve represents the results of McAlinden *et al.* [21]. (b) Same as (a) but for the $2s$ state. (c) Same as (a) but for $2p$ state.

figures, the present cross sections for all the states $(1s,2s,2p)$ are quite close to those due to McAlinden *et al.* [21], except at extreme forward ($\approx 0°$) angles (within the resolution of their figures) though their maximum cross sections (at zero angle) are always higher than the present ones. The qualitative nature of the two curves (the present and that

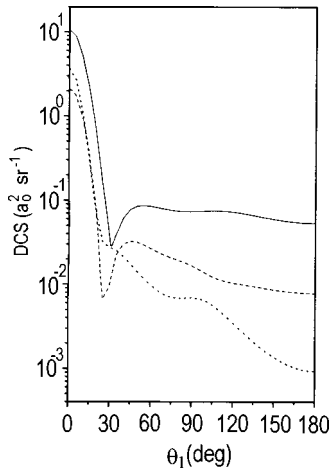

FIG. 3. Same as Fig. 1 but incident energy 25 eV.

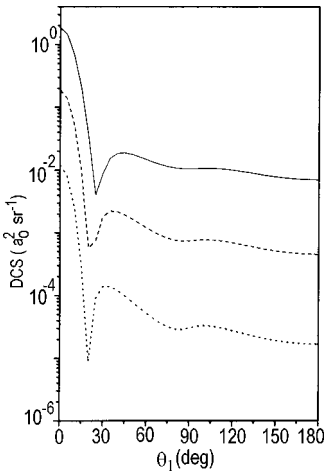

FIG. 4. DCS for Ps formation in 1*s* state for different incident energy. Solid curve for 50 eV, dashed line for 100 eV, and dotted line for 200 eV.

due to Ref. [21]) in Figs. 2(a)–2(c) is also more or less similar, although the peak and dip positions are slightly different.

Figure 3 displays similar DCS results (as in Fig. 1) but for higher value of the incident energy, e.g., E_i=25 eV. The figure reveals that at comparatively higher incident energy, the maximum value of the present DCS at forward angles is largest for the 1*s* state, smallest for the 2*s* state, and 2*p* lies in between, while for higher scattering angles, the magnitude of the partial DCS is in the increasing order for the 1*s*, 2*s*, and 2*p* states (i.e., $1s>2s>2p$). This behavior may be contrasted with that in Fig. 1 for lower incident energy. Comparison between Figs. 1 and 3 also indicates that the structures noted in all the partial DCS for lower incident energy (E_i=5 eV in Fig. 1) somewhat tend to smooth out with increasing incident energy (e.g., E_i=25 eV in Fig. 3).

Figures 4–6 exhibit the ground state (1*s*) as well as excited states ($2s,2p$) Ps formation DCS results for higher incident energies, e.g., 50, 100, and 200 eV. Comparing Figs. 1–3 and 4–6 it may be noted that the minima for the 1*s*, 2*s* as well as the kink for the 2*p* curves shift towards smaller angles with increasing incident energy. Further, a secondary

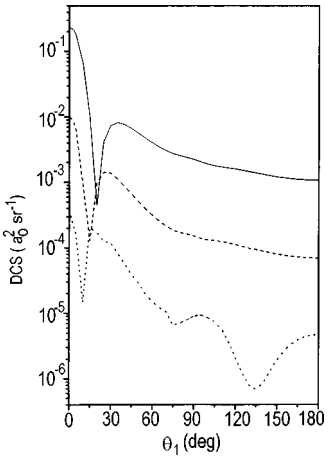

FIG. 5. Same as Fig. 4 but for Ps formation in 2*s* state.

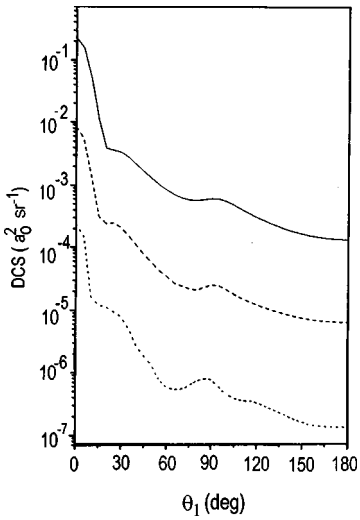

FIG. 6. Same as Fig. 4 but for Ps formation in 2*p* state.

maximum (minimum) starts appearing with increasing incident energy (vide Figs. 3–6), and gets more and more pronounced with increasing energy. Figures 4–6 indicate the prominent occurrence of these maxima at E_i=200 eV.

Anticipating that the Ps formation into the 1*s* state is most dominant at high incident energy, we now present in Fig. 7, some high-energy DCS results (e.g., for 300 and 500 eV) for the ground-state (1*s*) capture only. Figure 7 gives more clear evidence of the fact that with increasing incident energy, the signature of the double peak structure becomes more and more prominent.

The occurrence of the first minimum in the 1*s* and 2*s* differential curves (vide Figs. 1, 3–5, and 7) may be ascribed to the fact that the contributions from the attractive and the repulsive parts of the interaction potential to the scattering amplitude interfere destructively at this angle. Since with increasing incident energy both the amplitudes for attractive and repulsive parts become more and more peaked in the forward direction, the position of the minimum (due to the destructive interference between the two) shifts towards smaller angles as the energy increases. The minima for the

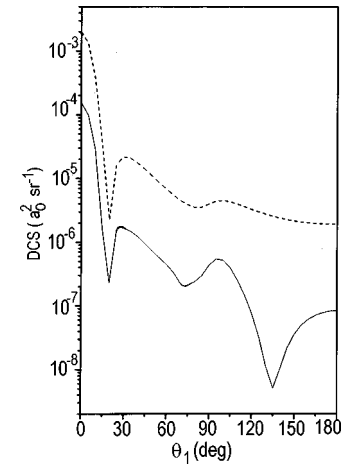

FIG. 7. Same as Fig. 4 but for higher incident energies. Dashed curve for 300 eV and solid curve for 500 eV.

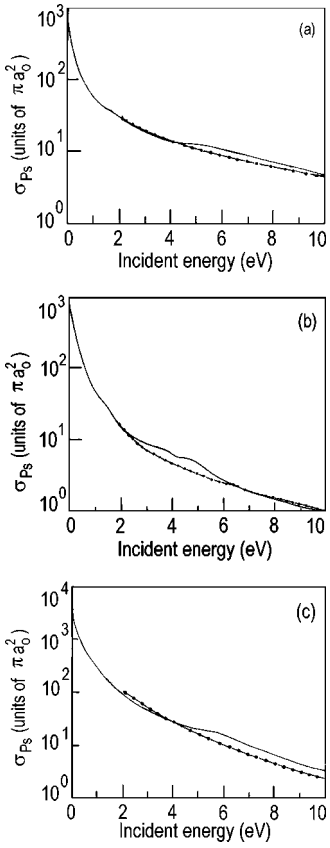

FIG. 8. (a) Partial total cross sections (units of πa_0^2) for positronium formation in 1*s* state for energy range 2–10 eV. Solid curve represents results due to McAlinden *et al.* [21] and the dashed dot curve represents present results. (b) Same as (a) but for the Ps formation in 2*s* state. (c) Same as (a) but for the Ps formation in 2*p* state.

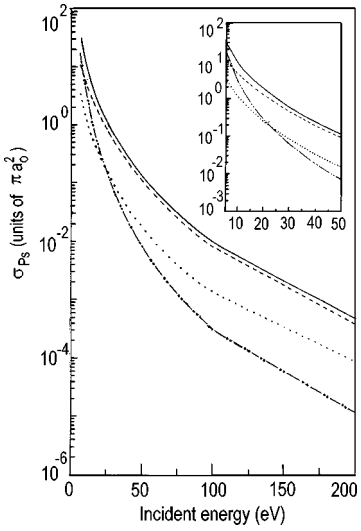

FIG. 9. Partial total cross sections (TCS) (units of πa_0^2) for positronium formation in $1s,2s,2p$ states and the integrated cross section $(1s+2s+2p)$ for the wider incident energy range (5–200 eV). Solid curve for integrated result, dashed curve for 1*s* state, dotted curve for 2*s* state, and dashed double dot curve for 2*p* state.

m-degenerate states occur at different scattering angles and as a result, the total differential cross sections for the 2*p* state do not exhibit such a minimum [33] but instead show a shoulderlike structure in that region. The appearance of the secondary minima at higher incident energies (e.g., Figs. 4, 5, and 7) for the 1*s* and 2*s* differential curves may be attributed to the second order effect. For the 2*p* state on the other hand, the prominent secondary minima appearing in the 1*s*, 2*s* differential curves (Figs. 5 and 7) are again somewhat suppressed resulting in some humplike structures (Fig. 6), due to the same reason as stated above for the first minimum, i.e., the maxima and minima of the $2p_0$ $(m=0)$ state occur at different scattering angles than those for the $2p_{\pm 1}$ $(m=\pm 1)$ states. As is also evident from Fig. 6, these secondary minima (for the 2*p* state) become more and more prominent with increasing incident energy, indicating the importance of the higher-order effects for higher incident energies. It should be pointed out here that no such secondary minimum occurs in the CBA [23] or in the OCBA [22] results even at very high incident energy (e.g., 300 eV).

The double peak structure occurring in the DCS of Ps formations in Figs. 4–7 could be attributed due to higher-order multiple scattering effect that has been accounted for through the eikonal phase factors.

Figures 8(a), 8(b), and 8(c) display the partial total cross sections (TCS) for capture into $1s,2s$, and $2p$ states for the lower incident energy regime (e.g., 2–10 eV). The corresponding results of McAlinden *et al.* [21] (from 0–10 eV) have also been included in the figures for comparison. It is revealed from the Figs. 8(a)–8(c) that the magnitude of the present TCS is in decreasing order for $1s,2s$, and $2p$ states in the high-energy regime (>20 eV), while in the lower-energy regime, the present partial TCS is found to be highest for the 2*p* state and lowest for the 2*s*, while the 1*s* lies in between. Similar features have also been noted by McAlinden *et al.* [vide Figs. 8(a)–8(c)] in the low-energy regime (0–10 eV).

It may be pointed out in this context that the present model is not suitable in the very low-energy regime and as such figures 8(a)–8(c) present the results only for 2–10 eV. On the other hand, the results obtained from the low-energy model (CPA) of McAlinden *et al.* [21] is expected to be reliable in the extreme low-energy regime (near zero energy).

Figure 9 demonstrates the present partial total cross sections (TCS) for the $1s,2s$, and $2p$ states for the energy regime 5–200 eV as well as the integrated cross sections $(1s+2s+2p)$. The inset of Fig. 9 illustrates the detailed behavior of the partial and the summed TCS in the low and intermediate energy regions (5–50 eV).

As may be noted from Fig. 9, all the partial TCS $(1s,2s,2p)$ as well as the summed total TCS $(1s+2s+2p)$ decrease monotonically with increasing incident energy. Figure 9 also reveals that for lower incident energy (e.g., 5–10 eV), the TCS for the 2*p* state is higher than those for 1*s* and 2*s* states (2*s* being lower than 1*s*) while in the intermediate energy regime (e.g., for 10–20 eV), the magnitude of the partial TCS follows the order $1s>2p>2s$ and beyond

TABLE I. Integral cross sections for positronium formation in the ground state in e^+-H^- ion collision. The numbers in square brackets indicate the power of 10 by which the entry is to be multiplied.

Incident energy (eV)	CBA		OCBA	CPA	CDEA
	Basu Choudhury *et al.*	Straton and Drachman	Straton *et al.*	McAlinden *et al.*	Present results
1		0.153[3]	82.5	57	53.07
10				~5(approx)	4.415
20	0.153[1]				0.125[1]
50	0.161[0]				0.101[0]
100	0.171[−1]	0.986[−2]			0.803[−2]
200	0.125[−2]				0.401[−3]

20 eV onwards (e.g., 20–200 eV), the partial TCS is in decreasing order for the 1*s*, 2*s*, and 2*p* states (i.e., $1s > 2s > 2p$).

For the sake of some numerical measure, we have displayed in Table I, the present integrated cross sections for the ground state (1*s*) Ps formation in the positron- negative hydrogen-ion collision along with the other corresponding existing theoretical results [21–23]. As may be noted from the table, the present CDEA cross sections compare well with the coupled pseudostate results of McAlinden *et al.* [21] at low incident energies (1–10 eV), the former (present) being always lower than the latter [21]. For higher incident energy (20–200 eV), on the other hand, the present CDEA results may be compared with the available CBA results of Basu Choudhury *et al.* [23] as well as the OCBA results of Straton *et al.* [22]. As is evident from the table, for the ground-state (1*s*) Ps formation, the present CDEA results are always smaller than the CBA or the OCBA results [22,23]. Table I further reveals that at intermediate energy (e.g., 20 eV), the present CDEA results agree well with the CBA results [23], however the discrepancy between the above two results increases with increasing incident energy. In fact even at $E_i = 200$ eV, the two results (CDEA and CBA) differ by more than a factor of 3. This discrepancy could again be attributed to the higher-order effects arising from the eikonal phase factors in the present model. Further, as is well known, for a rearrangement process the higher-order effects dominate at high incident energies.

IV. CONCLUSIONS

At low incident energies, the present (CDEA) Ps formation in 2*p* state is found to be the dominant process among the three states $1s, 2s, 2p$. This feature is in conformity with the low-energy calculations of McAlinden *et al.* [21]. At higher incident energy, on the other hand, the ground-state (1*s*) Ps formation dominates.

At high incident energy, the $1s, 2s$ DCS exhibit a distinct double peak structure that could be attributed to the higher-order effects arising from the eikonal phase factors. The signature of the double peak becomes more and more prominent with increasing incident energy indicating the increasing importance of the higher-order effects with incident energy. For the 2*p* state, however, the double peak structure is not so prominent as in the case of 1*s* and 2*s* states because of the *m*-degenerate states. No such double peak structure occurs in the Coulomb Born (CBA) results [23] even at high incident energy.

At low incident energies, the present CDEA results compare well with the results of McAlinden *et al.* [21] using coupled pseudostate approach, although the present results always give lower estimate of the latter [21]. At higher incident energies, on the other hand the present CDEA results lie always below the corresponding Coulomb Born results [23]. The discrepancy between the present CDEA and CBA [23] results arising due to higher-order effects however increases with increasing incident energy as is expected for a rearrangement process.

[1] G. Laricchia, P. Van Reeth, M. Sztuinska, and J. Moxom, J. Phys. B **35**, 2525 (2002).
[2] N. Overton, R. J. Mills, and P. G. Coleman, J. Phys. B **26**, 3951 (1993).
[3] M. Charlton and G. Laricchia, J. Phys. B **23**, 1045 (1990).
[4] L. M. Diana, P. G. Coleman, D. L. Brooks, P. K. Pendleton, and D. M. Norman, Phys. Rev. A **34**, 2731 (1986).
[5] D. Fromme, G. Kruse, W. Raith, and G. Sinapius, Phys. Rev. Lett. **57**, 3031 (1986).
[6] L. S. Fornari, L. M. Diana, and P. G. Coleman, Phys. Rev. Lett. **51**, 2276 (1983).
[7] J. W. Humberston, Adv. At. Mol. Phys. **22**, 1 (1986).
[8] T. C. Griffith, Adv. At. Mol. Phys. **22**, 37 (1986).
[9] *Positron Scattering in Gases*, edited by J. W. Humberston and M. R. C. McDowell (Plenum, New York, 1983), p. 206.
[10] N. K. Sarkar, M. Basu, and A. S. Ghosh, Phys. Rev. A **45**,

6887 (1992).
[11] M. Basu and A. S. Ghosh, Phys. Rev. A **43**, 4746 (1991), and the references cited therein.
[12] H. R. J. Walters, J. E. Blackwood, and M. T. McAlinden, in *New Directions in Antimatter Chemistry and Physics*, edited by C. M. Surko and F. A. Gianturco (Kluwer, Dordrecht, 2001), p. 173, and the references cited therein.
[13] R. N. Hewitt, C. J. Noble, and B. H. Bransden, J. Phys. B **25**, 557 (1992).
[14] M. T. McAlinden and H. R. J. Walters, Hyperfine Interact. **73**, 65 (1992).
[15] P. Chaudhuri and S. K. Adhikari, J. Phys. B **31**, 3057 (1998).
[16] N. C. Deb, D. S. F. Crothers, and D. Fromme, J. Phys. B **23**, L483 (1990).
[17] N. C. Deb, J. H. McGuire, and N. C. Sil, Phys. Rev. A **36**, 3707 (1987); **36**, 1082 (1987).
[18] M. J. Roberts, J. Phys. B **22**, 3315 (1989).
[19] D. R. Schultz and R. E. Olsen, Phys. Rev. A **38**, 1866 (1988).
[20] A. Igarashi and I. Toshima, Phys. Lett. A **164**, 70 (1992).
[21] M. T. McAlinden, J. E. Blackwood, and H. R. J. Walters, Phys. Rev. A **65**, 032715 (2002).
[22] Jack C. Straton and Richard J. Drachman, Phys. Rev. A **44**, 7335 (1991).
[23] K. Basu Choudhury, Arunima Mukherjee, and D. P. Sural, Phys. Rev. A **33**, 2358 (1986).
[24] L. H. Andersen, T. Andersen, and P. Hvelplund, Adv. At., Mol., Opt. Phys. **38**, 155 (1998).
[25] D. S. F. Crothers, Proc. Phys. Soc. London **91**, 855 (1967).
[26] D. Ghosh and C. Sinha, Phys. Rev. A **68**, 062701 (2003).
[27] S. Chandrasekhar, Astrophys. J. **100**, 176 (1944).
[28] A. Messiah, *Quantum Mechanics* (North-Holland, Amsterdam, 1966), Vol. 1, p. 481.
[29] L. S. Gradshteyn and I. M. Ryzhik, *Tables and Integrals, Series and Products* (Academic, New York, 1980), Vol. 310(2), Sec. 8, p. 933.
[30] R. R. Lewis, Jr., Phys. Rev. **102**, 537 (1956).
[31] R. Biswas and C. Sinha, Phys. Rev. A **50**, 354 (1994).
[32] B. Nath and C. Sinha, J. Phys. B **33**, 5525 (2000).
[33] N. C. Sil, B. C. Saha, H. P. Saha, and P. Mondal, Phys. Rev. A **19**, 655 (1979).